European Journal of Drug Metabolism and Pharmacokinetics (2023) 48:455–462
https://doi.org/10.1007/s13318-023-00831-x

SHORT COMMUNICATION

Re-examining Naloxone Pharmacokinetics After Intranasal and Intramuscular Administration Using the Finite Absorption Time Concept

Athanasios A. Tsekouras[1,2] · **Panos Macheras**[2,3]

Accepted: 9 May 2023 / Published online: 2 June 2023

Abstract

Background and Objectives Naloxone for opioid overdose treatment can be administered by intravenous injection, intramuscular injection, or intranasal administration. Published data indicate differences in naloxone pharmacokinetics depending on the route of administration. The aim of this study was to analyze pharmacokinetic data in the same way that we recently successfully applied the concept of the finite absorption time in orally administered drug formulations.

Methods Using the model equations already derived, we performed least squares analysis on 24 sets of naloxone concentration in the blood as a function of time.

Results We found that intramuscular and intranasal administration can be described more accurately when considering zero-order absorption kinetics for finite time compared with classical first order absorption kinetics for infinite time.

Conclusions One-compartment models work well for most cases. Two-compartment models provide better details, but have higher parameter uncertainties. The absorption duration can be determined directly from the model parameters and thus allow an easy comparison between the ways of administration. Furthermore, the precise site of injection for intramuscular delivery appears to make a difference in terms of the duration of the drug absorption.

Key Points

Finite absorption time affects oral pharmacokinetics and its modeling.

Emergency overdose antidote naloxone, administered intravenously, intramuscularly, or intranasally, follows similar models.

One- and two-compartment model-fitting to several sets of data prove them adequate and better than classical models.

✉ Panos Macheras
macheras@pharm.uoa.gr

1 Department of Chemistry, Laboratory of Physical Chemistry, National and Kapodistrian University of Athens, Athens, Greece

2 PharmaInformatics Unit, Research Center ATHENA, Athens, Greece

3 Faculty of Pharmacy, Laboratory of Biopharmaceutics Pharmacokinetics, National and Kapodistrian University of Athens, Athens, Greece

1 Introduction

Opioid overdose is a dynamic public health epidemic. Naloxone HCl injection has been used for nearly 50 years to reverse the effects of opioids. Naloxone acts as a non-selective and competitive opioid antagonist. Its binding affinity is highest for the μ-opioid receptor, then the δ-opioid receptor, and lowest for the κ-opioid receptor [1].

Naloxone is administered intravenously, intramuscularly, and intranasally [2]. In the community setting, individuals who lack the medical expertise to titrate a dose to achieve a desired response are using the intranasal and intramuscular products [2]. This common use of naloxone aims to counter slow or shallow breathing in opioid overdose before emergency treatment is available.

A number of pharmacokinetic studies [3–11] have been carried out for the non-compartmental analysis of naloxone after intranasal and intramuscular administration. These publications are mainly focused on the relative bioavailability of naloxone upon intranasal and intramuscular administration. We recently found [12] that naloxone pharmacokinetics after intranasal and intramuscular administration can be described with the recently developed physiologically-based finite time pharmacokinetic (PBFTPK) models [13–15]. In this work, we analyze all available data published in the

literature [3–11] by performing compartmental analysis applying classical approaches as well as PBFTPK models. These models were developed for orally administered drugs with time restrictions for intestinal (≤ 5 h) and colon drug absorption (≤ 30 h) [13–15]. Due to the limited residence time of nasal sprays on the nostril mucosa, it was thought that the PBFTPK models could also be applied for the analysis of naloxone intranasal data. In addition, the absorption of drugs after intramuscular administration is well known to depend on the injection site as well as on physiological factors, e.g., the depth of fat in gluteal injections. Accordingly, classical and PBFTPK models were applied to naloxone intranasal and intramuscular pharmacokinetic studies to elucidate naloxone absorption characteristics in terms of the type of kinetics, the input rate(s), and the duration of absorption.

The aim of this study was to explore the utility and applicability of PBFTPK modeling to intramuscular and intranasal pharmacokinetic data in the same way that we recently successfully applied the concept of the finite absorption time in orally administered drug formulations.

2 Methods

From the nine pharmacokinetic naloxone studies reported here [3–11], we analyzed the six studies [4, 5, 7, 8, 10, 11] which included the measured naloxone blood concentrations, $C_b(t)$, as a function of time, t, post-dose. Twenty-four datasets were found in the six studies that met this criterion. The $C_b(t)$ plots were digitized by transferring the published figures to the Windows utility MS Paint, reading off the coordinates of axes ranges and data points and performing linear interpolation to recover the data shown in the published papers They were then analyzed with a variety of models assuming one- and two-compartment disposition. Two types of naloxone input rates were considered assuming one-compartment model disposition for the intranasal and intramuscular administration, namely, classical first-order absorption of infinite duration (Eq. S1) or zero-order absorption for finite absorption time (FAT), τ, considering one (Eq. S2), two, or three consecutive absorption stages [13–15]; All the equations used are reported in the Supplementary Information.

The number of parameters determined varied from 3 for the simplest models to 7 for the most complex ones. The least-squares method was implemented within the programming environment of Igor by WaveMetrics [14, 15] for all fitting work. Parameter uncertainties, co-variances, and correlations between them were determined to help assess the quality of each fit. Fit residuals, i.e., differences between experimental and calculated points, were also plotted as an additional criterion for the quality of each fit.

3 Results

3.1 Intravenous Data

The best fits using the two-compartment model equation (Eq. S6) for the two datasets [5, 8] are presented in Fig. 1.

3.2 Intramuscular Data

The analysis of eight sets of naloxone intramuscular data is presented in Fig. 2. Only one out of eight datasets follows classical first-order absorption kinetics, Fig. 2b. In this case, volunteers received 0.8 mg of naloxone as an injection to the

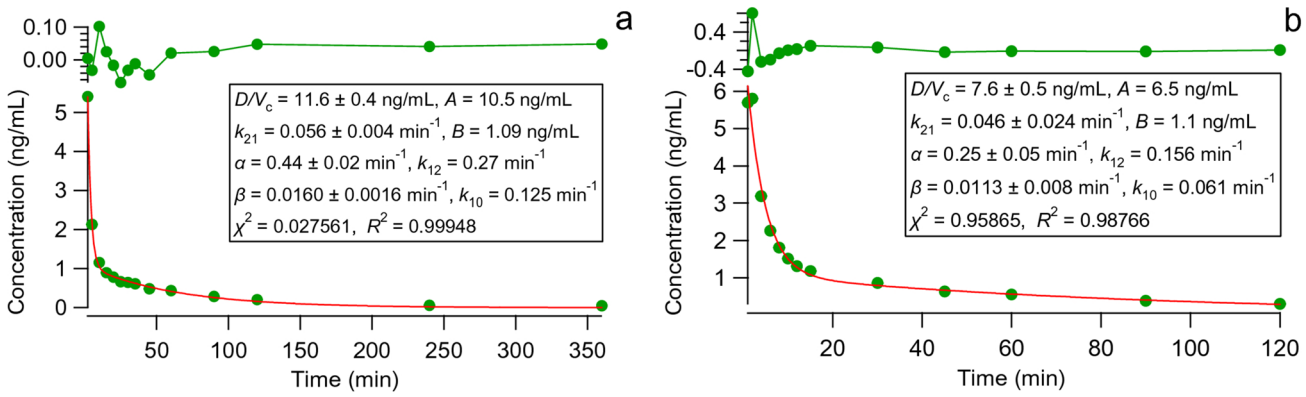

Fig. 1 Best fits of Eq. S6 to intravenous data upon administration of a bolus naloxone dose of 0.4 mg. *The top part of each plot* is the residual plot; key: **a** [8], **b** [5]; symbols: D dose, V_c volume of central compartment, k_{12}, k_{21}, k_{10} rate micro-constants in two compartment models, α, β hybrid rate constants of distribution and elimination, respectively, A, B pre-exponential factors, χ^2 sum of squares of deviations, R^2 correlation coefficient

deltoid muscle while receiving remifentanil by a target-controlled infusion; the average value of t_{max} was found equal to 7.75 min [7]. Seven datasets (Fig. 2a, c, d, e, f, g, h) were described nicely by the PBFTPK models [13–15]. Three of them (Fig. 2a, g, h) were described by a two-compartment model and four of them (Fig. 2c, d, e, f) by a one-compartment model. All fitting results based on classical first-order absorption with either one- or two-compartment model kinetics are reported in the Supplementary Information.

The findings presented in Fig. 2 are tabulated in Table 1, which shows the estimates for the duration of drug absorption stages, the site of injection, and the dose administered for seven naloxone intramuscular administrations described by PBFTPK models [14, 15].

3.3 Intranasal Data

The analysis of the 14 datasets is presented in Fig. 3. Only 2 of them are best described by a two-compartment model, while 12 follow one-compartment model disposition.

4 Discussion

4.1 Intravenous Data

Both iv datasets [5, 8] were best described by a two-compartment model (Fig. 1). Quite similar β estimates, 0.016 ± 0.0016 and 0.011 ± 0.008 min,$^{-1}$ were found for the two datasets analyzed. Moderate values, 4.9 and 3.4, were found for the ratio of the micro-constants k_{12}, k_{21} in the two studies [5, 8], indicating a rather quick approach to equilibrium between the central and the peripheral compartments.

4.2 Intramuscular Data

Based on the data presented in Table 1, the mean termination of naloxone absorption, τ, regardless of the site of injection or the dose administered, is 10 ± 5 min, excluding the second very slow absorption stage of Fig. 2h. For the studies including deltoid muscle administration, regardless of the dose administered, the mean termination of naloxone absorption is 4.7 min (mean of two datasets); the corresponding values for naloxone injection to gluteus maximus (one dataset) and anterolateral aspect of the thigh (four datasets) are 14.4 and 11.8 min, respectively. These results are associated with the proximity of the injection sites to the vasculature of the relevant tissues. It seems that the injection to the deltoid muscle results in shorter termination of naloxone absorption compared to the gluteus maximus and the anterolateral aspect of the thigh injections. However, the variation of time to maximum concentration, interpreted as FAT in this study, following different sites of injection is very well known [16].

4.3 Intranasal Data

Twelve intranasal datasets follow one-compartment model disposition and two datasets follow two-compartment model disposition, Fig. 3. However, in all the cases studied and regardless of the disposition model, it was found that naloxone absorption terminates at a specific time τ; this corresponds to the FAT of the PBFTPK models developed recently [13–15]. The estimate of the mean for the duration of naloxone absorption using all 14 datasets shown in Fig. 3 is 16 ± 3 min; it should be noted that this estimate is based on all the different types of naloxone nasal administration and doses used in the studies [4, 5, 7, 9, 10]. It is also noted that all the naloxone intranasal profiles exhibit a single concentration maximum, which corresponds to naloxone absorption from the nasal epithelium. The absence of a second peak rules out the absorption of naloxone from the gastrointestinal tract due to swallowed particles.

The analysis presented here was based on the mean data reported in the literature. A better analysis could be based on a mixed effects modeling approach with a common single model, e.g., the most frequently used two-compartment model. Unfortunately, this modeling exercise requires individual data, which are not reported in the literature.

The present successful analysis of the intranasal and intramuscular data using PBFTPK models shows the applicability and utility of these models. This is also the case in a recent study [17] on the complementarity of PBPK (bottom–up) and PBFTK (top–down) approaches; the latter revealed the physically sound termination of the drug absorption process in contrast to exponentially reaching the 100% plateau at infinite time generated by the PBPK models. The PBFTPK models were also sufficiently powerful for the analysis of the complex absorption kinetics of mavoglurant [12], which has so far been analyzed with stochastic approaches.

However, a word of caution is required since the pharmacodynamic (PD) aspects of naloxone injections or intranasal administration were not examined here. In fact, the

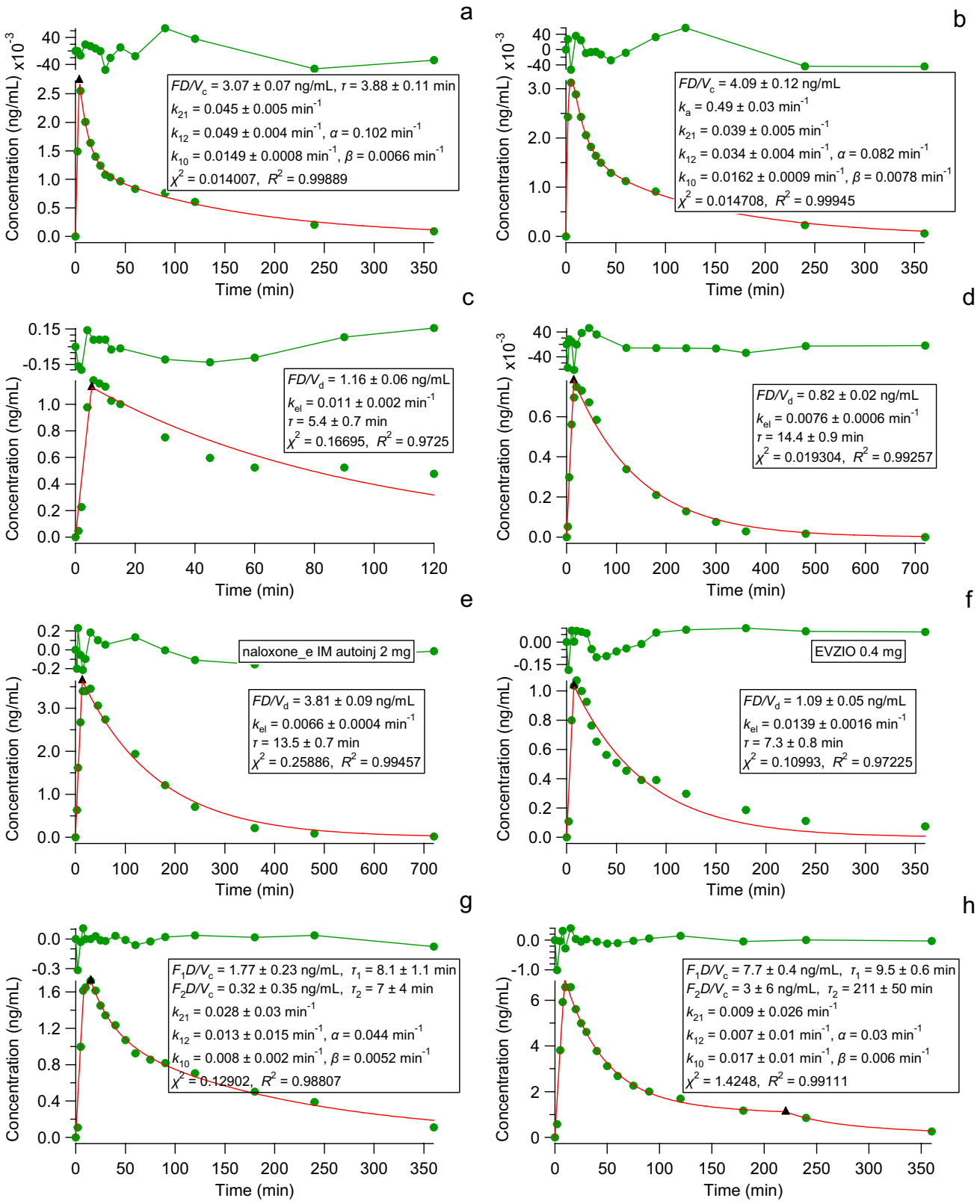
a
Concentration (ng/mL) x10^-3
Time (min)
FD/Vc = 3.07 ± 0.07 ng/mL, τ = 3.88 ± 0.11 min
k21 = 0.045 ± 0.005 min^-1
k12 = 0.049 ± 0.004 min^-1, α = 0.102 min^-1
k10 = 0.0149 ± 0.0008 min^-1, β = 0.0066 min^-1
χ^2 = 0.014007, R^2 = 0.99889
b
Concentration (ng/mL) x10^-3
Time (min)
FD/Vc = 4.09 ± 0.12 ng/mL
ka = 0.49 ± 0.03 min^-1
k21 = 0.039 ± 0.005 min^-1
k12 = 0.034 ± 0.004 min^-1, α = 0.082 min^-1
k10 = 0.0162 ± 0.0009 min^-1, β = 0.0078 min^-1
χ^2 = 0.014708, R^2 = 0.99945
c
Concentration (ng/mL)
Time (min)
FD/Vd = 1.16 ± 0.06 ng/mL
kel = 0.011 ± 0.002 min^-1
τ = 5.4 ± 0.7 min
χ^2 = 0.16695, R^2 = 0.9725
d
Concentration (ng/mL) x10^-3
Time (min)
FD/Vd = 0.82 ± 0.02 ng/mL
kel = 0.0076 ± 0.0006 min^-1
τ = 14.4 ± 0.9 min
χ^2 = 0.019304, R^2 = 0.99257
e
Concentration (ng/mL)
Time (min)
naloxone_e IM autoinj 2 mg
FD/Vd = 3.81 ± 0.09 ng/mL
kel = 0.0066 ± 0.0004 min^-1
τ = 13.5 ± 0.7 min
χ^2 = 0.25886, R^2 = 0.99457
f
Concentration (ng/mL)
Time (min)
EVZIO 0.4 mg
FD/Vd = 1.09 ± 0.05 ng/mL
kel = 0.0139 ± 0.0016 min^-1
τ = 7.3 ± 0.8 min
χ^2 = 0.10993, R^2 = 0.97225
g
Concentration (ng/mL)
Time (min)
F1D/Vc = 1.77 ± 0.23 ng/mL, τ1 = 8.1 ± 1.1 min
F2D/Vc = 0.32 ± 0.35 ng/mL, τ2 = 7 ± 4 min
k21 = 0.028 ± 0.03 min^-1
k12 = 0.013 ± 0.015 min^-1, α = 0.044 min^-1
k10 = 0.008 ± 0.002 min^-1, β = 0.0052 min^-1
χ^2 = 0.12902, R^2 = 0.98807
h
Concentration (ng/mL)
Time (min)
F1D/Vc = 7.7 ± 0.4 ng/mL, τ1 = 9.5 ± 0.6 min
F2D/Vc = 3 ± 6 ng/mL, τ2 = 211 ± 50 min
k21 = 0.009 ± 0.026 min^-1
k12 = 0.007 ± 0.01 min^-1, α = 0.03 min^-1
k10 = 0.017 ± 0.01 min^-1, β = 0.006 min^-1
χ^2 = 1.4248, R^2 = 0.99111

◂**Fig. 2** Blood concentration-time data, and best fits after intramuscular administration at different intramuscular injection sites of different naloxone doses. *The top part of each plot* is the residual plot. Key: **a** [8, 12], **b** [7], **c** [5], **d** [4], **e** [10], **f** [11], **g** [11], **h** [11]; symbols: F, F_1, F_2 bioavailable fractions, V_d volume of distribution, τ, τ_1, τ_2 duration of absorption stage, k_a first order absorption rate constant, k_e elimination rate constant; other symbols are defined in Fig. 1. The *triangle* denotes the end of the absorption process. Panel **a** has appeared in [12], but is included here for completeness

penetration of naloxone to the brain of rats is very rapid, due to its lipophilic nature, followed by a rapid decline of naloxone quantities in the brain [18]. Parallel profiles for naloxone quantities in the brain and naloxone blood levels were recorded in rats a long time ago [18], while the nasal to brain delivery of naloxone in humans has been studied recently [19]. Several comprehensive reviews for naloxone penetration into the human brain following intranasal administration have been published (e.g., [20]). In this context, PBFTPK-PD models could be launched for the analysis of relevant data such as those found in a very recent study of intramuscular and intranasal administration of epinephrine [21].

5 Conclusion

The utilization of PBFTPK models [13–15] enabled us to assess for the first time the termination of naloxone absorption from the intramuscular and intranasal formulations. The results demonstrate that the completion of naloxone absorption is more rapid when injected into the deltoid muscle compared to other routes of intramuscular administration or via the intranasal route. This is an additional positive property of the intramuscular administration apart from the better bioavailability of naloxone compared to the intranasal route reported previously [8]. All the above are helpful for the optimization of the use of naloxone in the community setting due to the urgent need to counter breathing problems in opioid overdose. It is advised that the FAT concept and the relevant PBFTPK models [13–15] be combined with pharmacodynamic recordings and models to elucidate the pharmacokinetic–pharmacodynamic profile of naloxone upon intramuscular and intranasal administration.

Table 1 Intramuscular administration of naloxone

References	Dose (mg)	Injection site	FAT (min)
8	0.8	Deltoid	3.9
5	0.4	Deltoid	5.4
4	0.4	Gluteus maximus	14.4
10	2	Anterolateral aspect of the thigh	13.5
11	0.4	Anterolateral aspect of the thigh	7.3
11	0.8	Anterolateral aspect of the thigh	15
11	2	Anterolateral aspect of the thigh	9.5

Estimates for the duration of naloxone absorption stage(s) in the seven studies described by PBFTPK models [14, 15]

The results from Fig. 2b are not included because they are best described by the classical model for which FAT is not defined

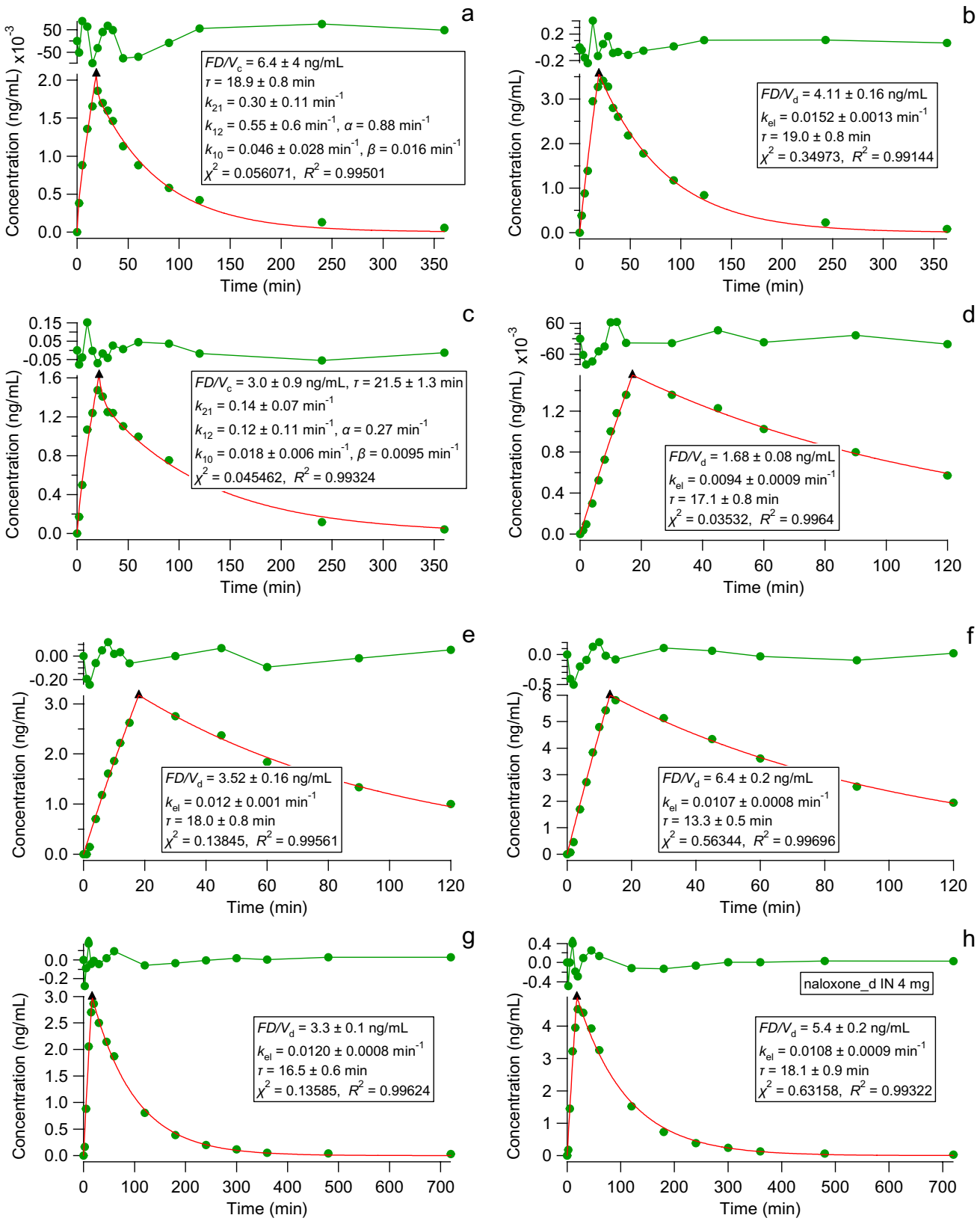

Fig. 3 Blood concentration-time data, and best fits after intranasal administration of different doses of naloxone. *The top part of each plot* is the residual plot. The *triangle* denotes the end of the absorption process. Panel **a** has appeared in [12], but is included here for completeness. Key: **a**, **b** [8]; **c** [7]; **d**, **e**, **f** [5]; **g**, **h**, **I**, **j** [4]; **k**, **l**, **m**, **n** [10]; symbols defined in Figs. 1 and 2

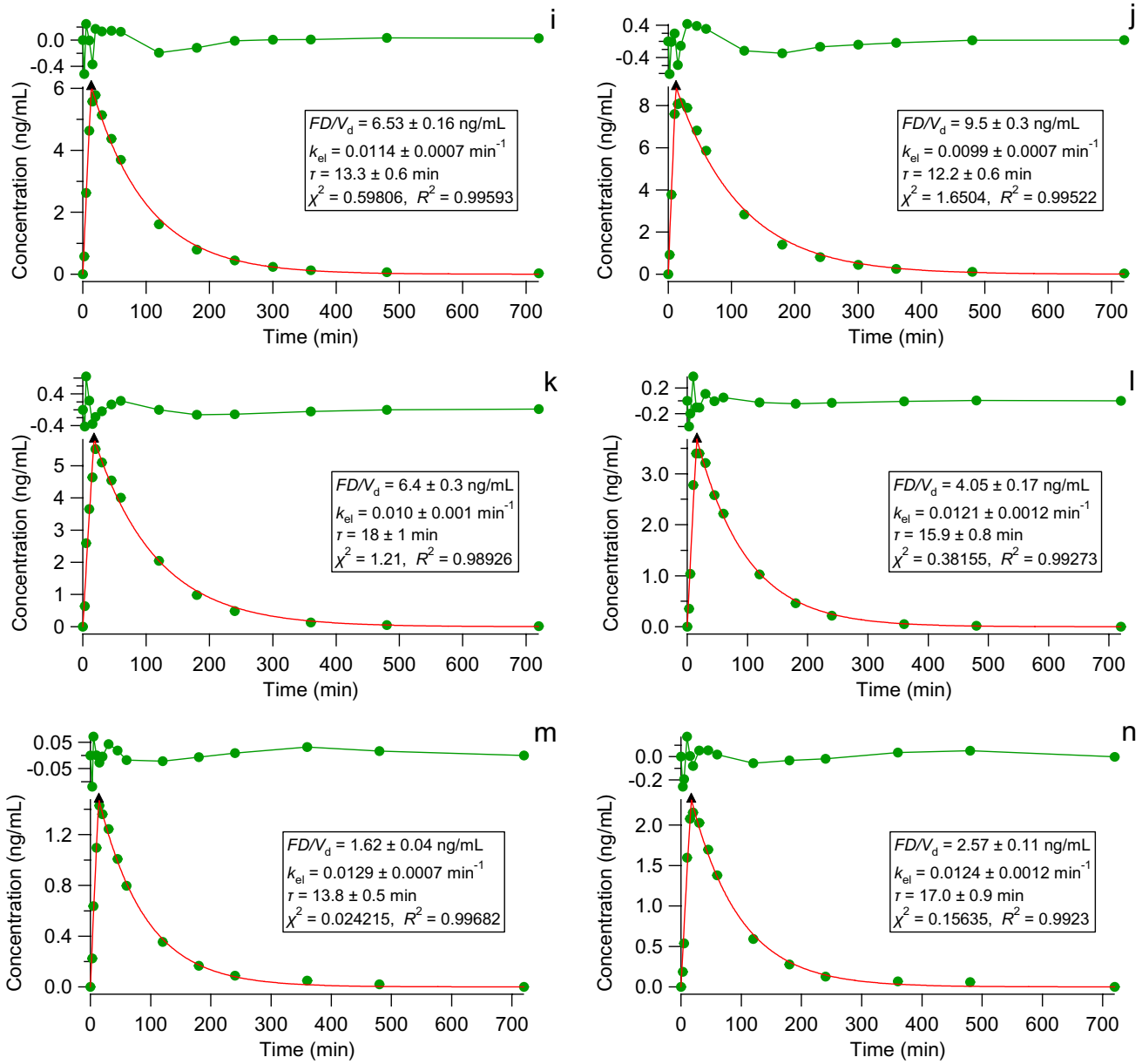

Fig. 3 (continued)

Supplementary Information The online version contains supplementary material available at https://doi.org/10.1007/s13318-023-00831-x.

Declarations

Funding This research did not receive any specific grant from funding agencies in the public, commercial, or not-for-profit sectors.

Competing interests The authors declare no competing interests.

Ethics approval Not applicable.

Consent to participate Not applicable.

Consent for publication Not applicable.

Data availability The datasets analyzed during the current study are available in the publications referenced.

Code availability Custom written software is available upon request.

Author contributions PM conceived the work and wrote the first draft. AAT did the data retrieval and analysis. Both authors revised and approved the manuscript.

References

1. Malenka RC, Nestler EJ, Hyman SE, Sydor A, Brown RY (eds.). Molecular neuropharmacology: a foundation for clinical

neuroscience, 2nd ed. New York: McGraw-Hill Medical, pp. 190–191, 287; 2009.
2. US Food and Drug Administration. Kaleo briefing on naloxone HCl. Joint Meeting of the Anesthetic and Analgesic Drug Products and the Drug Safety and Risk Management Advisory Committees October 5, 2016 kaleo, Inc. Briefing Dossier.
3. Dowling J, Isbister GK, Kirkpatrick CMJ, Naidoo D, Graudins A. Population pharmacokinetics of intravenous, intramuscular, and intranasal naloxone in human volunteers. Ther Drug Monit. 2008;30:490–6. https://doi.org/10.1097/FTD.0b013e3181816214.
4. Krieter P, Chiang N, Gyaw S, Skolnick P, Crystal R, Keegan F, Aker J, Beck M, Harris J. Pharmacokinetic properties and human use characteristics of an FDA-approved intranasal naloxone product for the treatment of opioid overdose. J Clin Pharmacol. 2016;56:1243–53. https://doi.org/10.1002/jcph.759.
5. McDonald R, Lorch U, Woodward J, Bosse B, Dooner H, Mundin G, Smith K, Strang J. Pharmacokinetics of concentrated naloxone nasal spray for opioid overdose reversal: Phase I healthy volunteer study. Addiction. 2017;113:484–93. https://doi.org/10.1111/add.14033.
6. Tylleskar I, Skulberg AK, Nilsen T, Skarra S, Jansook P, Dale O. Pharmacokinetics of a new, nasal formulation of naloxone. Eur J Clin Pharmacol. 2017;73:555–62. https://doi.org/10.1007/s00228-016-2191-1.
7. Skulberg AK, Tylleskar I, Nilsen T, Skarra S, Salvesen O, Sand T, Loftsson T, Dale O. Pharmacokinetics and -dynamics of intramuscular and intranasal naloxone: an explorative study in healthy volunteers. Eur J Clin Pharmacol. 2018;74:873–83. https://doi.org/10.1007/s00228-018-2443-3.
8. Skulberg AK, Asberg A, Khiabani HZ, Rostad H, Tylleskar I, Dale O. Pharmacokinetics of a novel, approved, 1.4-mg intranasal naloxone formulation for reversal of opioid overdose—a randomized controlled trial. Addiction. 2019;114:859–67. https://doi.org/10.1111/add.14552.
9. Dietze P, Jauncey M, Salmon A, Mohebbi M, Latimer J, van Beek I, McGrath C, Kerr D. Effect of intranasal vs intramuscular naloxone on opioid overdose: a randomized clinical trial. JAMA Netw Open. 2019;2: e1914977. https://doi.org/10.1001/jamanetworkopen.2019.14977.
10. Krieter PA, Chiang N, Gyaw S, McCann DJ. Comparison of the pharmacokinetic properties of naloxone following the use of FDA-approved intranasal and intramuscular devices versus a common improvised nasal naloxone device. J Clin Pharmacol. 2019;59:1078–84. https://doi.org/10.1002/jcph.1401.
11. US Food and Drug Administration, Evzio (naloxone hydrochloride injection) Auto-injector for intramuscular or subcutaneous use, FDA, 4001455; 2016.
12. Tsekouras AA, Macheras P. The Finite Absorption Time (FAT) Concept en route to PBPK modeling and pharmacometrics. J Pharmacokinet Pharmacodyn. 2022. https://doi.org/10.1007/s10928-022-09832-w.
13. Macheras P, Chryssafidis P. Revising pharmacokinetics of oral drug absorption: I Models based on biopharmaceutical/physiological and finite absorption time concepts. Pharm Res. 2020;37:187. https://doi.org/10.1007/s11095-020-02894-w. (Erratum, Pharm Res. 2020;37:206. https://doi.org/10.1007/s11095-020-02935-4).
14. Chryssafidis P, Tsekouras AA, Macheras P. Re-writing oral pharmacokinetics using physiologically based finite time pharmacokinetic (PBFTPK) models. Pharm Res. 2022;39:691–701. https://doi.org/10.1007/s11095-022-03230-0.
15. Macheras P, Tsekouras AA. Revising oral pharmacokinetics, bioavailability and bioequivalence based on the finite absorption time concept. Cham: Springer; 2023. https://doi.org/10.1007/978-3-031-20025-0.
16. Zuidema J, Pieters FAJM, Duchateau GSMJE. Release and absorption rate aspects of intramuscularly injected pharmaceuticals. Int J Pharm. 1988;47:1–12. https://doi.org/10.1016/0378-5173(88)90209-8.
17. Wu D, Tsekouras AA, Macheras P, Kesisoglou F. Physiologically based pharmacokinetic models under the prism of the finite absorption time concept. Pharm Res. 2023;40:419–29. https://doi.org/10.1007/s11095-022-03357-0.
18. Ngai SH, Berkowitz BA, Yang JC, Hempstead J, Spector S. Pharmacokinetics of naloxone in rats and in man: basis for its potency and short duration of action. Anesthesiology. 1976;44:398–401. https://doi.org/10.1097/00000542-197605000-00008.
19. Giunchedi P, Gavini E, Bonferoni MC. Nose-to-Brain Delivery. Pharmaceutics. 2020;12:138. https://doi.org/10.3390/pharmaceutics12020138.
20. Johansson J, Hirvonen J, Lovró Z, Ekblad L, Kaasinen V, Rajasilta O, Helin S, Tuisku J, Sirén S, Pennanen M, Agrawal A, Crystal R, Vainio PJ, Alho H, Scheinin M. Intranasal naloxone rapidly occupies brain mu-opioid receptors in human subjects. Neuropsychopharmacology. 2019;44:1667–73. https://doi.org/10.1038/s41386-019-0368-x.
21. Tanimoto S, Kaliner M, Lockey RF, Ebisawa M, Pesco Koplowitz L, Koplowitz B, Lowenthal R. Pharmacokinetic and pharmacodynamic comparison of epinephrine, administered intranasally and intramuscularly. Ann Allergy Asthma Immunol. 2023;130:508–14. https://doi.org/10.1016/j.anai.2022.10.024.